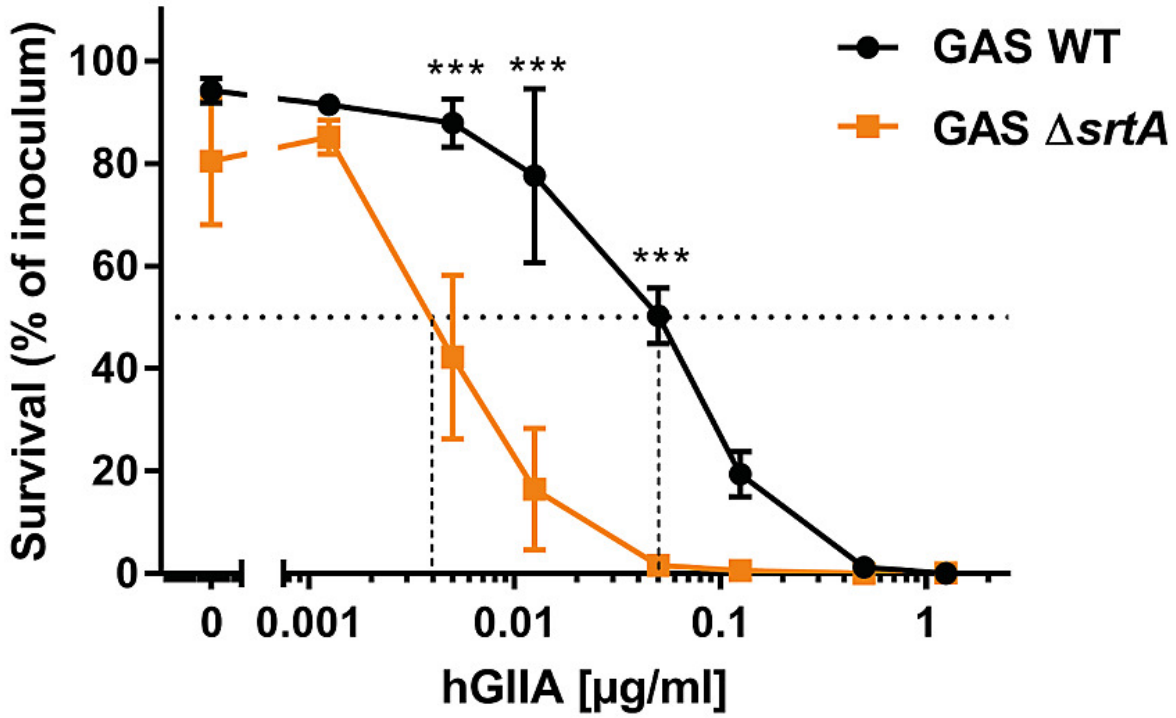

S1 Fig. GAS M1T1 5448 is killed by hGIIA in a dose-dependent manner. Mutation of srtA renders 5448 more susceptible to hGIIA killing. Data represent mean +/- SD of three independent experiments. ***, $p \leq 0.001$.

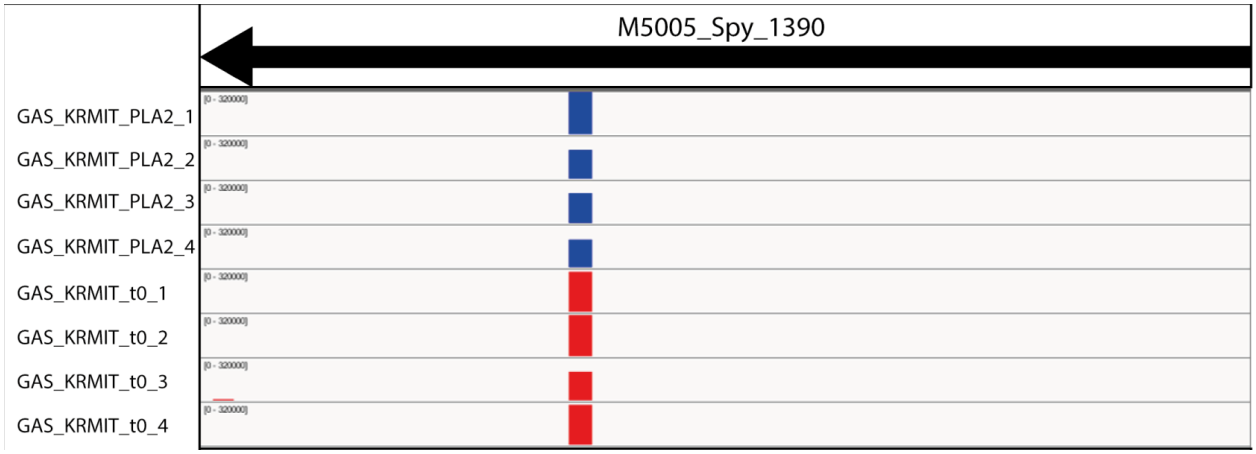

S2 Fig. Biased transposon insertions in *M5005_Spy_1390*. Unusual high number of transposon insertions at one location in the gene *M5005_Spy_1390*.

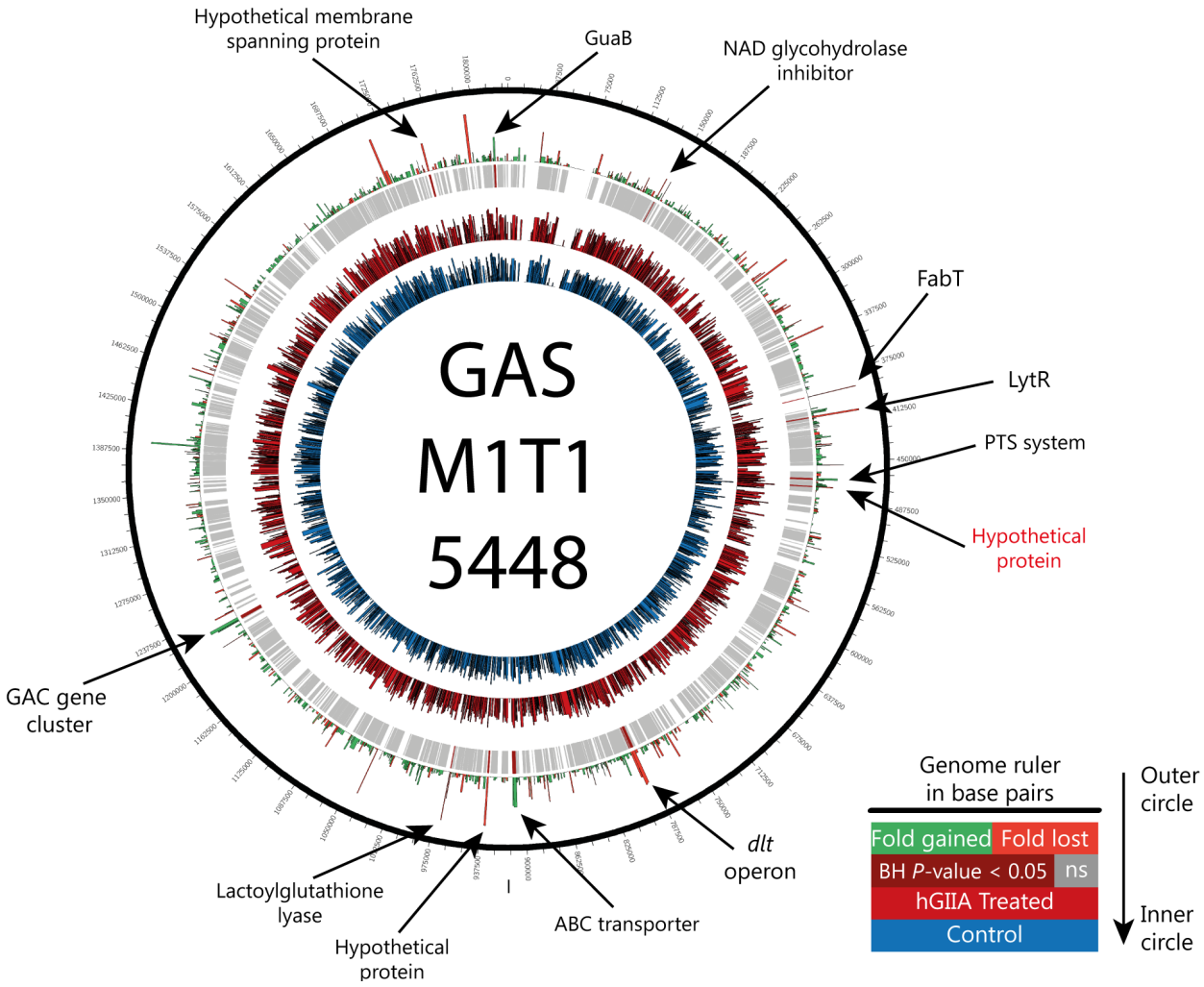

S3 Fig. Tn-seq results. Circos respresentation of the Tn-seq data. Each bar in the inner two circles, where blue is control and red the hGIIA treated, represent the average RKPM value of a gene. The following to circles represent the BH corrected p-value and the fold change in log of the hGIIA treated samples vs control samples. Red bars indicate a fold a respective fold decrease and green bars a respective fold increase of transposon insertions. The gene highlighted in red is M5005_Spy_1390, which showed significant fold change due to unusual high transposon insertions at one specific point in the gene.

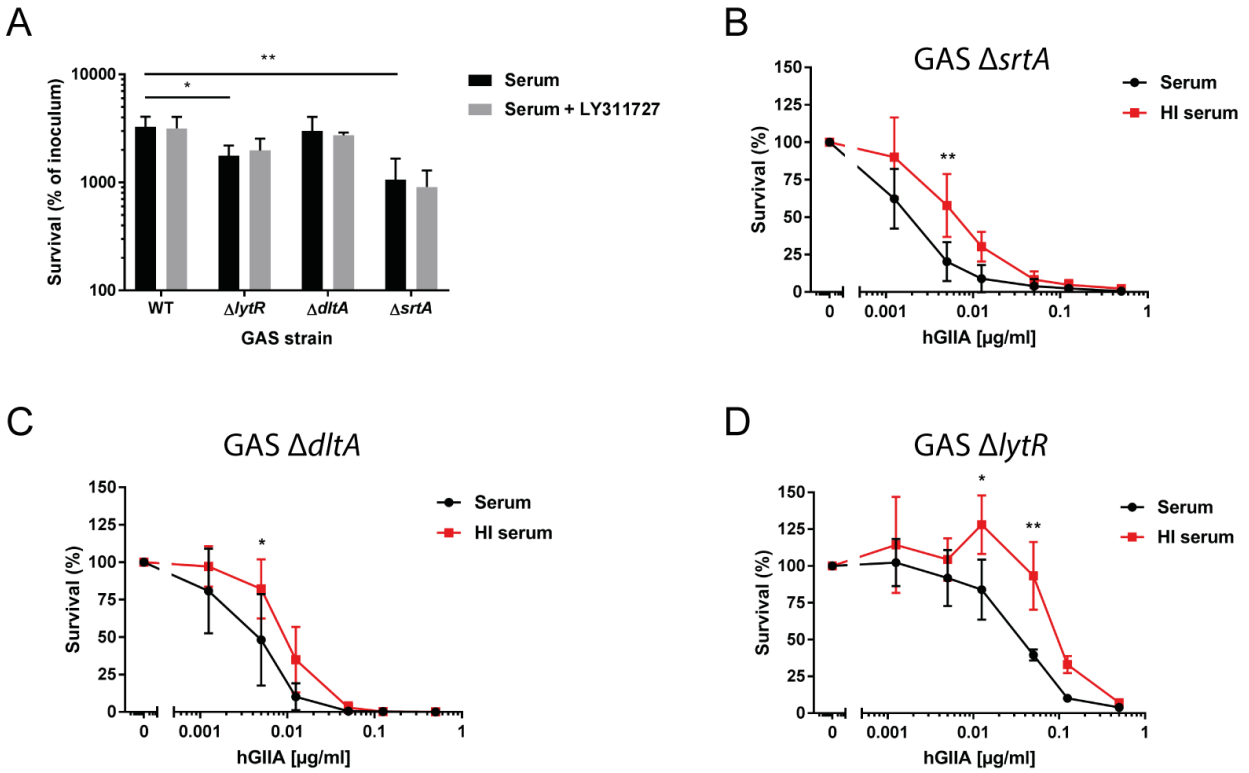

S4 Fig. Serum contains a heat-labile factor that increases hGIIA efficacy. (A) Endogenous hGIIA in serum does not affect growth of GAS. Mutation of lytR and srtA does attenuate GAS growth independent of hGIIA. This heat-labile factor also affects killing of the (B) srtA, (C) dltA, and (D) lytR mutants. Data represent mean +/- SD of three independent experiments, *, $p \leq 0.05$; **, $p \leq 0.01$.

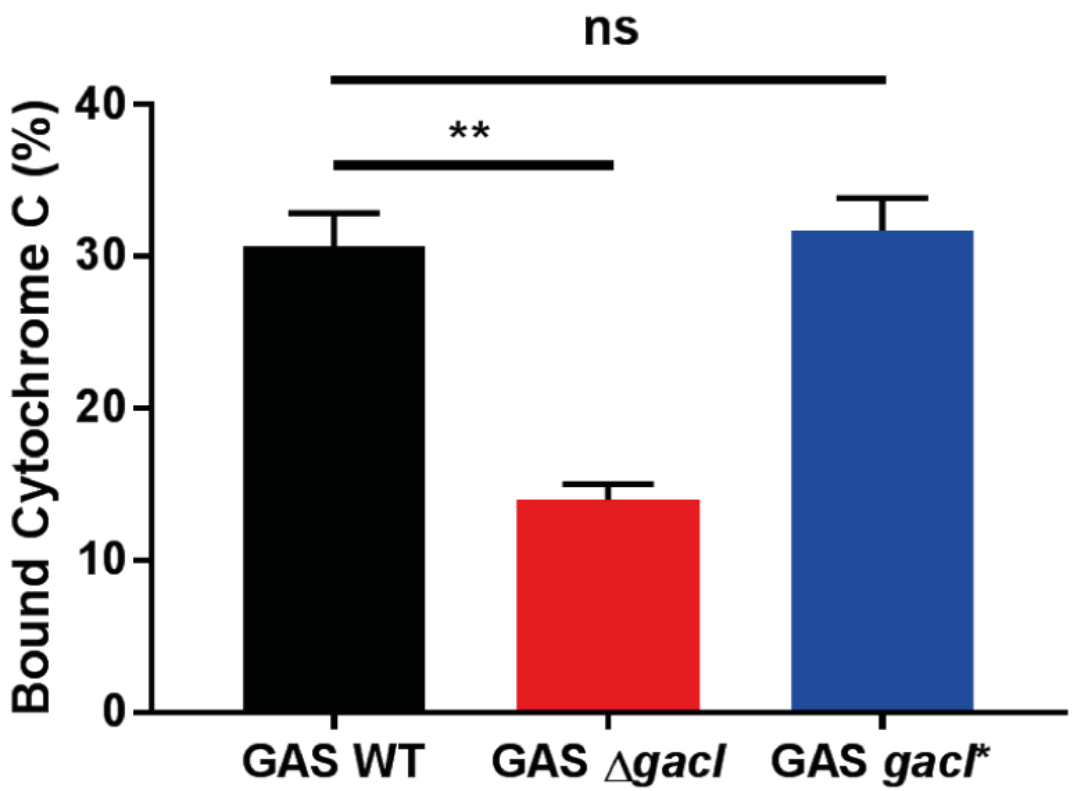

S5 Fig. Surface charge of GAS WT and GAS ΔgacI. Deletion of gacI affects surface charge of GAS as determined in cationic cytochrome c binding assay. Data represent mean +/- SD of three independent experiments. ns = not significant, **, $p \leq 0.01$.

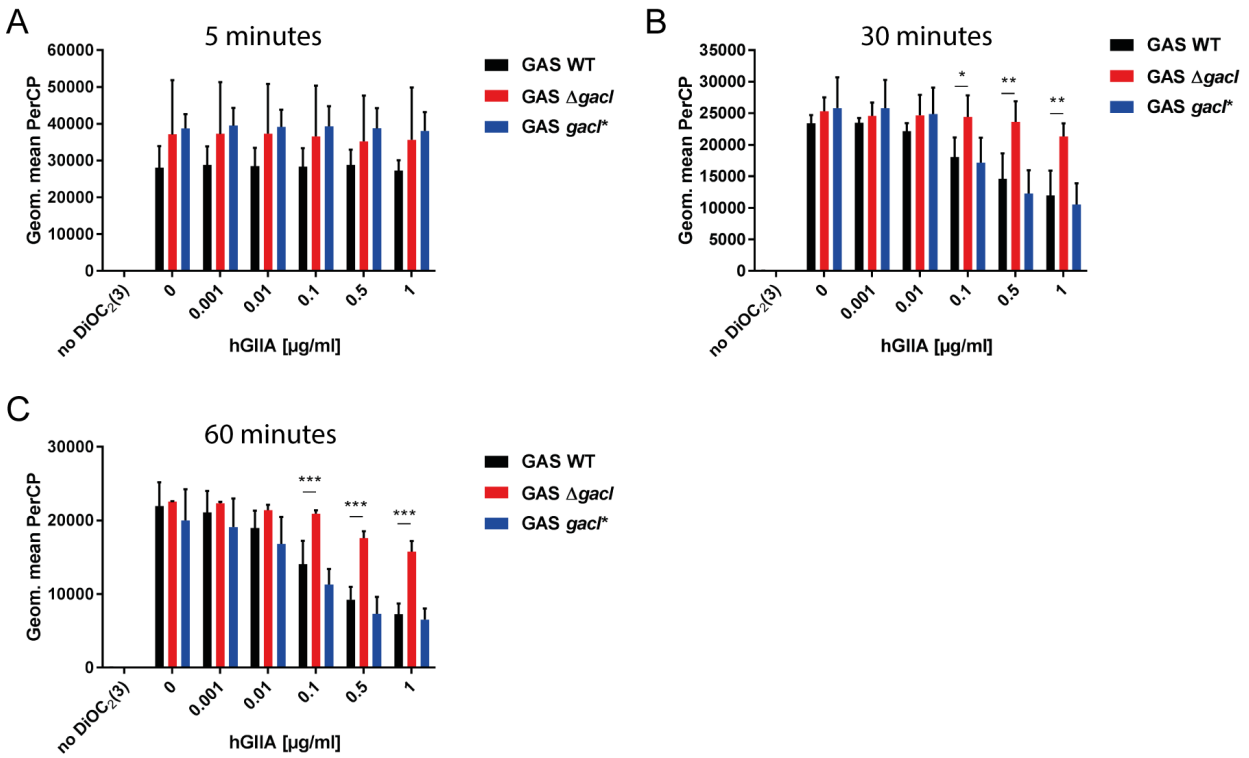

S6 Fig. Three additional time points for DiOC2(3) measurements. The effect of hGIIA stress on GAS membrane potential after (A) 5 minutes, (B) 30 minutes and (C) 60 minutes. Data represent mean +/- SD of three independent experiments. *, $p \leq 0.05$; **, $p \leq 0.01$; ***, $p \leq 0.001$.

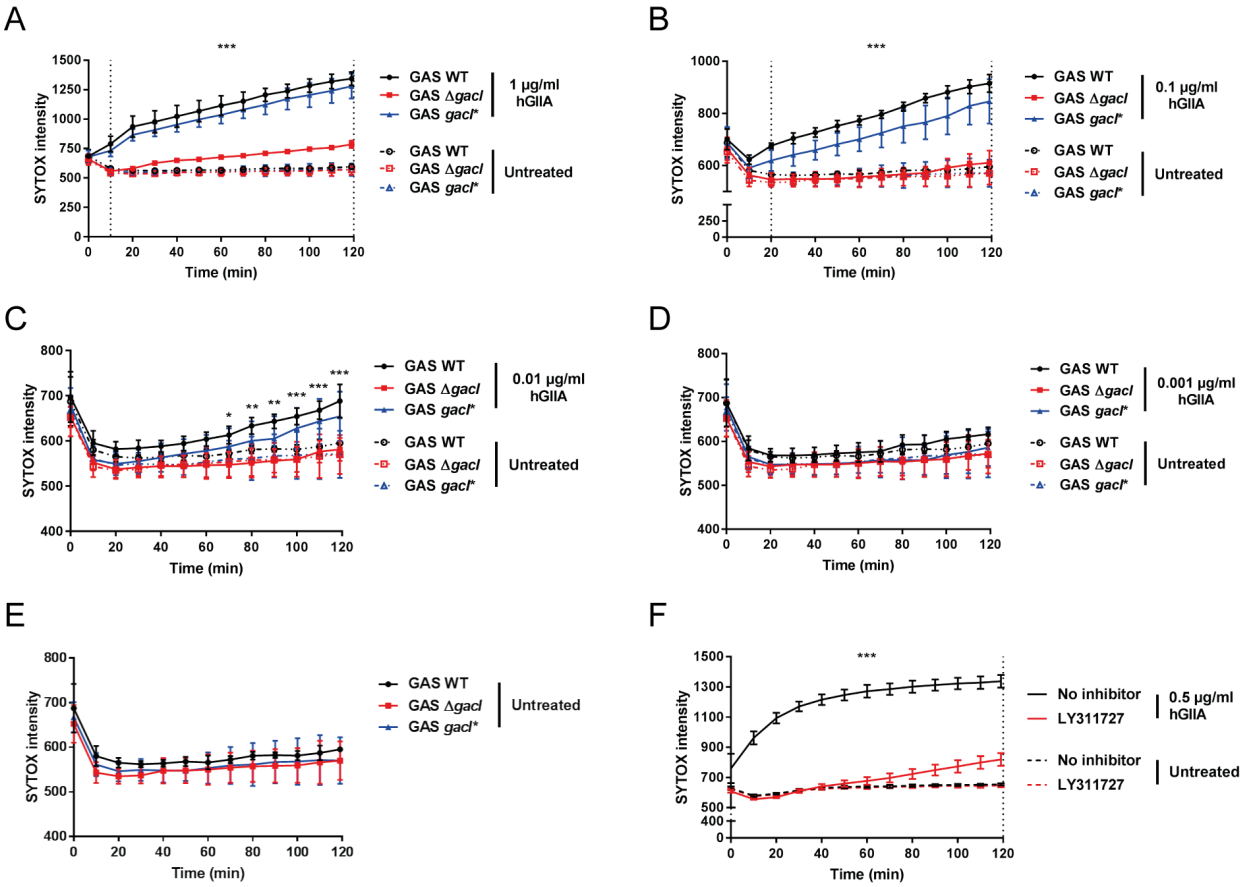

S7 Fig. Kinetics of the SYTOX influx in intact GAS strains. SYTOX influx measured over 120 minutes when GAS strains are incubated with, (A) 1, (B) 0.1, (C) 0.01, (D) 0.001, and (E) 0 µg/ml hGIIA. (F) Addition of 500 µM LY311727 to 0.5 µg/ml hGIIA prevents SYTOX influx. Data represent mean +/- SD of three independent experiments. *, $p \leq 0.05$; **, $p \leq 0.01$; ***, $p \leq 0.001$.

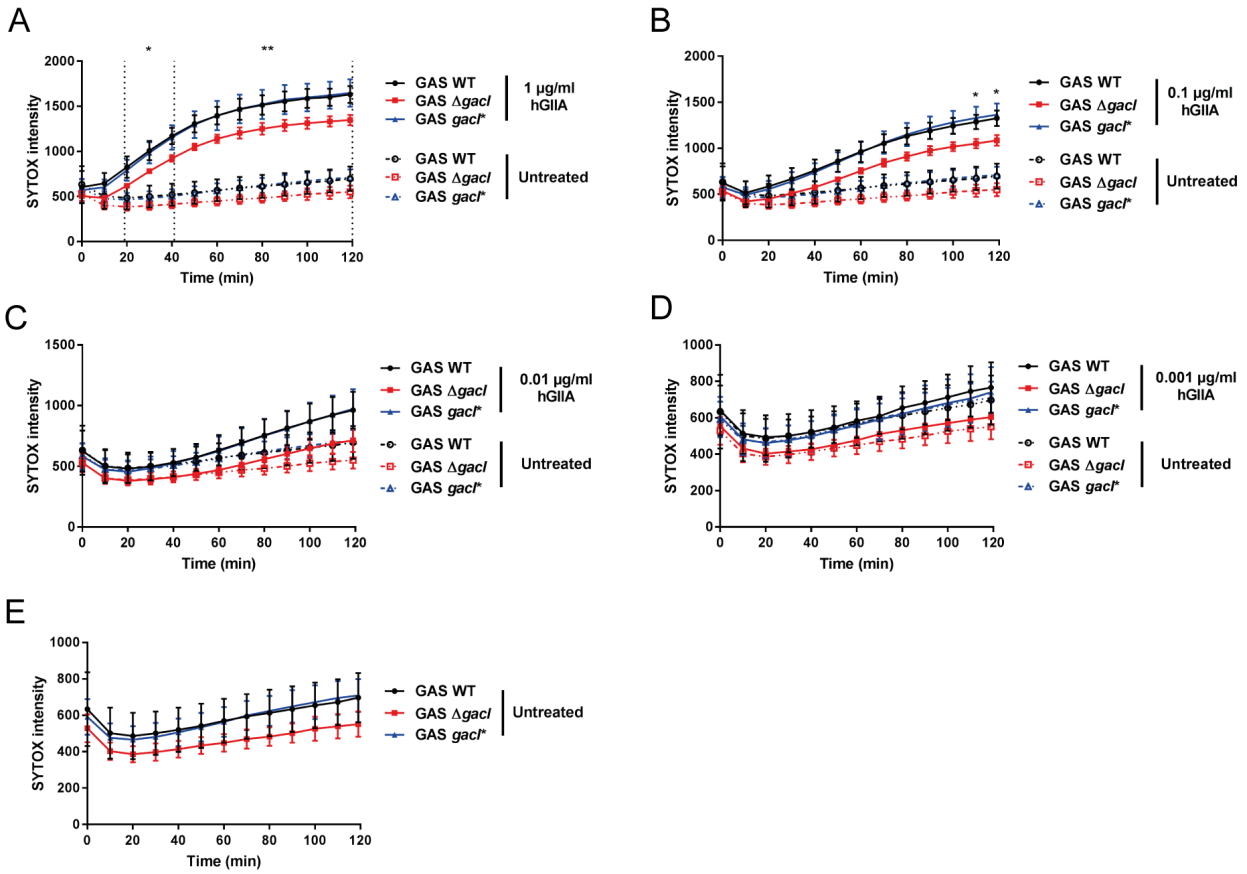

S8 Fig. Kinetics of the SYTOX influx in protoplast GAS strains. SYTOX influx measured over 120 minutes when protoplast GAS strains are incubated with (A) 1, (B) 0.1, (C) 0.01, (D) 0.001, and (E) 0 µg/ml hGIIA. Data represents mean +/- SD of three independent experiments. *, $p \leq 0.05$; **, $p \leq 0.01$.

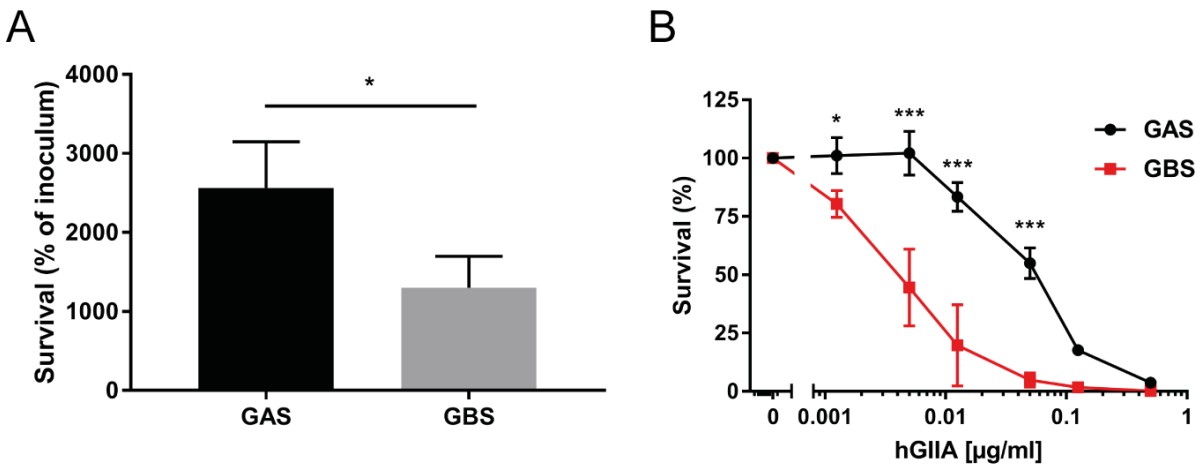

S9 Fig. Gas and GBS are differently affected by human serum. (A) GAS grows faster in human serum compared to GBS. (B) GBS is more susceptible to hGIIA-spiked in serum compared to GAS. Data represent mean +/- SD of three independent experiments. *, $p \leq 0.05$; ***, $p \leq 0.001$.

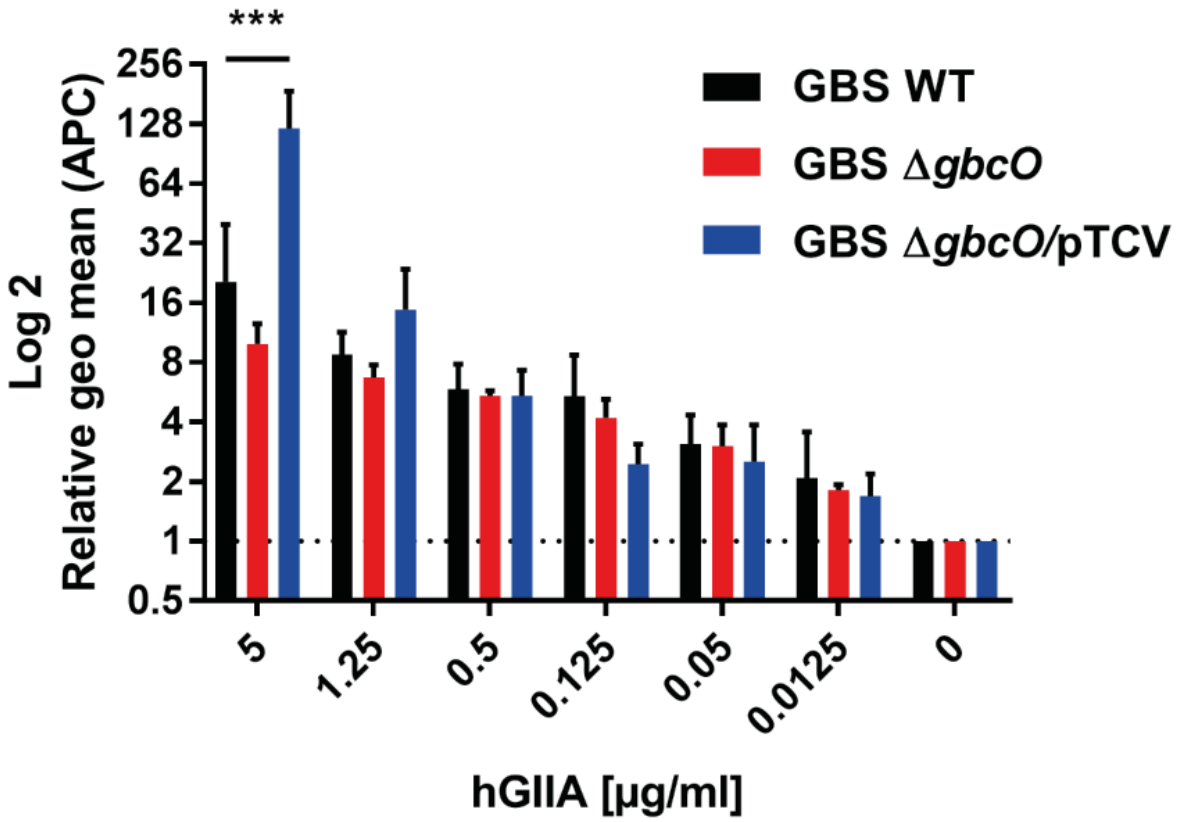

S10 Fig. HGIIA surface binding to GBS. No significant difference in relative hGIIA surface binding of GBS WT and GBS ΔgbcO. Data represent mean +/- SD of three independent experiments. ***, $p \leq 0.001$.